Absorption-based fiber optic surface plasmon resonance sensor: a theoretical evaluation

Anuj K. Sharma, B.D. Gupta*

Department of Physics, Indian Institute of Technology Delhi, New Delhi 110016, India

Received 12 December 2003; received in revised form 29 January 2004; accepted 6 February 2004

Available online 21 April 2004

Abstract

In this paper, an optical absorption based fiber optic surface plasmon resonance (SPR) sensor has been studied theoretically. The theoretical treatment is based on Kretschmann's SPR theory and the Lorentz model that expresses a damped harmonic oscillator is included in the treatment for optical absorption in the sensing layer. The optical source considered is an un-polarized collimated beam. The light is coupled to the fiber using a micro scope obj ective that focuses the beam at the center of the input face of the fiber. The effects of the parameters related to the sensing region, the light source and the optical fiber on the sensitivity and the operating range of the SPR sensor have been studied with the help of numerical calculations and computer simulations. It has been found that the excitation frequency in absorption-based fiber optic SPR sensor is an important parameter. The sensitivity is better for the lower off-resonance excitation frequency. The sensitivity and the operating range of the sensor are better for large value of the core diameter. The optimization of numerical aperture of the fiber, film thickness and the length of the sensing region is required to achieve the maximum sensitivity. Further, the increase in the extinction coefficient of the sample increases the sensitivity of the sensor while the decrease in the width of its absorption spectrum increases the sensitivity. The sensitivity and the operating range of the sensor are better for small values of the refractive index of the absorbing sample.

Keywords: Optical fiber; Surface plasmon resonance; Absorption; Sensor

1. Introduction

In 1983, Liedberg et al. [1] were the first to point out that the phenomenon of optical excitation of surface plasmons is very useful for optical sensing. Since then, there have been several studies and developments in the field of surface plasmon resonance (SPR) sensors. SPR is a surface-sensitive analytical method for chemical and biochemical sensing [2-6] that is based on measuring changes in the refractive index on the noble metal surface. A unique feature of SPR sensors is a strong localization of the electromagnetic field of the surface plasmon. Therefore, it is possible to achieve a very high concentration of this field in the sensing medium and to reach extremely high sensitivity.

In the early years after the release of SPR phenomenon by Kretschmann [7-9], few attempts were made to develop the SPR sensor based on the optical absorption effect. But these were with very limited improvement because the concerned practical theory described in terms of the relation between the reflectance and the incident angle (SPR curve) did not exist. Recently, Kurihara and Suzuki [10] and Kurihara et al. [11] presented a general and practical theory of optical absorption-based SPR sensors. In their work, they used the Kretschmann's SPR theory and the optical absorption in the sensing layer was included by the Lorentz model that expresses a damped harmonic oscillator.

The optical absorption effect stands for the change in both imaginary as well as real part of the refractive index of the sensing layer. In the conventional SPR sensor the change in the real part of the refractive index of the sensing layer is measured from the SPR curves. The absorption based SPR sensor makes use of changes in imaginary part of the refractive index of the sensing layer for chemical and biochemical sensing. The labeling based on the optical absorption using absorption materials such as dye molecules is more useful for preparing high sensitivity SPR sensor. In the absorption-based labeling, the amplification of surface plasmon waves (SPW) can be controlled by the concentration of absorption materials. In their work, Kurihara

and Suzuki [10] described the theoretical background of the absorption-based SPR for future development of chemical and biochemical sensors. A three layer Fresnel equation relating p-polarization in which the sensing system consisting of a prism-metal-absorbing sensing layer was considered. The SPR curves were obtained as a function of frequency of light source and the thickness of the metal film on the prism base. The theory of the optical absorption-based SPR sensor was explained by the simulation of the SPR curves using optical parameters related to a silver-metal-based SPR sensor.

The prism based SPR sensors are bulky, require expensive optical equipments and remote sensing is difficult. These shortcomings of prism based SPR sensor were removed by replacing prism by an optical fiber [12-15]. Optical fibers offer many other advantages also. They are perceived as being safer for in vivo use since the signal is optical and there is no electromagnetic interference. Since optical fibers avoid cross-talk, a small, compact, multi-sensing SPR fiber probe is possible. In this paper we present an optical absorption based fiber optic SPR sensor. The theoretical approach is similar to that of Kurihara and Suzuki [10]. The optical source considered is an un-polarized collimated beam and the light is coupled to the fiber using a microscope objective focusing the beam at the center of the input face of the fiber. The effects of the parameters related to the sensing region, the light source and the optical fiber on the sensitivity and the operating range of the sensor have been studied theoretically with the help of numerical calculations and computer simulations.

2. Theory

2.1. Background

We consider three-layer Fresnel equations for p- and s-polarization in which the sensing system consists of a prism-metal-sensing layer (Fig. 1). When the p- or s-polarized light is incident at an angle θ, the reflectance R of the light is given by the following three-layer Fresnel equations as follows:

$$R = \left| \frac{rp_m + r_{ms} \exp(2ik_{mz}d)}{1 + r_{pm} r_{ms} \exp(2ik_{mz}d)} \right|^2 \quad (1)$$

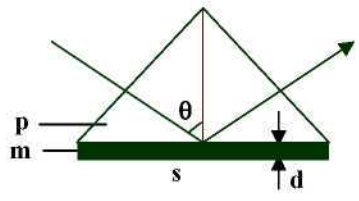

Fig. 1. Kreschmann configuration of a prism-metal-sensing layer interface. The glass prism, the metallic film, and the sensing layer are labeled p, m, and s, respectively. θ is the incident angle, and d is the thickness of the metallic film.

For p-polarization

$$r_{pm} = r^{p}_{pm} = \frac{k_{pz}\varepsilon_m - k_{mz}\varepsilon_p}{k_{pz}\varepsilon_m + k_{mz}\varepsilon_p} \quad (2)$$

and

$$r_{ms} = r^{p}_{ms} = \frac{k_{mz}\varepsilon_s - k_{sz}\varepsilon_m}{k_{mz}\varepsilon_s + k_{sz}\varepsilon_m} \quad (3)$$

For s-polarization

$$r_{pm} = r^{s}_{pm} = \frac{k_{pz} - k_{mz}}{k_{pz} + k_{mz}} \quad (4)$$

and

$$r_{ms} = r^{s}_{ms} = \frac{k_{mz} - k_{sz}}{k_{mz} + k_{sz}} \quad (5)$$

Further

$$k_z = \left(\varepsilon_j \omega \frac{c^2}{c^2} - k_x^2 \right)^{1/2} \quad (6)$$

$$k_x = \sqrt{\varepsilon_j} \frac{\omega}{c} \sin\theta \quad (7)$$

where prism, metal layer and sensing layer are denoted by p, m and s letters, respectively; r_{pm} and r_{ms} are the amplitude reflectances given by Fresnel formulae for prism-metal and metal-sensing layer interfaces, respectively; ε_j is the dielectric constant of the mediumj; kj_z the wave vector component perpendicular to the interface in medium j; k_x the component of the wave vector parallel to the interface; d the thickness of the metallic film; ω the angular frequency of the incident light and c is the velocity of light. The dielectric constant of the prism layer is given by

$$\varepsilon_p = n_p^2 \quad (8)$$

where n_p is the refractive index of the prism material. Using Drude model, the dielectric constant of the metal layer is given as

$$\varepsilon_m = \varepsilon^{\infty}_m \left(\frac{\omega_p^2}{\omega(\omega + i\omega_d)} \right) \quad (9)$$

where ω is the frequency of incident light; ω_p the plasma frequency; ωd the damping frequency and ε^{∞}_m is the background dielectric constant at infinite frequency.

If N represents the number of absorption oscillators per unit volume then the dielectric constant of the sensing layer is given by the Lorentz model as

$$\varepsilon_s = \varepsilon_s^{\infty} + \frac{Ne^2}{m_e \varepsilon_0} \frac{f}{(\omega_0^2 - \omega^2 - i\omega\gamma)} \quad (10)$$

with

$$\omega_0 = \frac{2\pi c}{\lambda_{max}} \quad (11)$$

$$\gamma = |\omega_0| = 2\pi c \frac{\Delta\lambda_{max}}{\lambda^2_{max}} \quad (12)$$

and

$$N = 10^3 N_A C \tag{13}$$

where C is the molar concentration of absorption oscillators; N_A the Avagadro's number; e^° the background dielectric constant of the sensing layer; fis the oscillator strength and is a function of molar extinction coefficient; λ_{max} and $\lambda\lambda_{max}$ are the absorption maximum wavelength and the full width at half-maximum of absorption spectrum of the sensing layer sample, respectively; ω0 is the absorption frequency; ε0 the permittivity of vacuum; e the elementary charge and m_e is the electron mass. In order to obtain separately the real and imaginary parts of the refractive index of the sensing layer, we take the case when

$$n_s + iK_s = \sqrt{\varepsilon_s} \tag{14}$$

Assuming C « 1 , Eq. (10) can be written as

$$n_s = \sqrt{\varepsilon_s^\infty}\left[1 + C\frac{10^3 e^2 N_A}{2\varepsilon_0 m_s \omega_0}\frac{f_{\varepsilon>0}^2 - \omega^2}{(\omega_0^2 - \omega^2)^2 + (\omega\gamma)^2}\right] \tag{15}$$

and

$$\kappa_s = C\frac{10^3 e^2 N_A}{2\sqrt{\varepsilon_s^\infty} m_e \varepsilon_0}\frac{\omega\gamma}{(\omega_0^2 - \omega^2)^2 + (\omega\gamma)^2} \tag{16}$$

According to Krestchmann's theory [15], Eq. (1) for p-polarization can be transformed to

$$R_p = 1 - \frac{4k''_{0p}k''_{Rp}}{|k - k_{mp}|^2} \tag{17}$$

with

$$k_{mp} = k'_{mp} + ik''_{mp} = k_{0p} + k_{Rp} \tag{18}$$

$$k_{0p} = k'_{0p} + ik''_{0p} = \frac{\omega}{c}\sqrt{\frac{\varepsilon_m \varepsilon_s}{\varepsilon_m + \varepsilon_s}} \tag{19}$$

and finally,

$$k_{Rp} = k'_{Rp} + ik''_{Rp} = -\frac{\omega}{c}(r^p_{pm})_{k_x=k_0}\left(\frac{\varepsilon_m \varepsilon_s}{\varepsilon_m + \varepsilon_s}\right)^{3/2}\exp\left[i\frac{And}{\lambda}\left\{\frac{\varepsilon_m}{(\varepsilon_m + \varepsilon_s)^{1/2}}\right\}\right] \tag{20}$$

where k_{mp} is the complex wave-vector of surface plasmon waves generated under the Kretschmann ATR condition; k_{0p} is the complex wave-vector of the SPW at the metal-sensing layer interface in the absence of the prism; kR_p is the perturbation to $k0_p$ in the presence of the prism. The imaginary parts of the $k0_p$ and KR_p are the intrinsic and radiative damping, respectively. The former represents the Joule loss in the metal and the latter represents the leakage loss of the SPW back into the prism. For s-polarization, the expression for reflectance R_s is given by

$$R_S = A\left[1 - \left\{\frac{B + C(k_x - D)}{(k_x - D)^2 + E^2}\right\}\right] \tag{21}$$

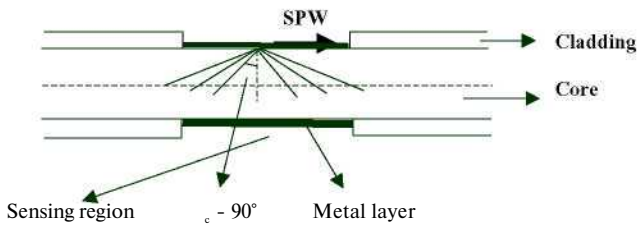

Fig. 2. Illustration of the SPR fiber optic sensor.

where

$$A = \left|\frac{1}{\sqrt{s}}\right|^2 \tag{22}$$

$$B = -2|k_{Rs}|^2 + 2(s' - 1)k'_{Rs} + 2|k_{Rs}|^2 - 2s''k'_{Rs}k''_{Rs} \tag{23}$$

$$C = 2[(s' - 1)k'_{Rs} - s''k''_{Rs}] \tag{24}$$

$$D = k'_{Rs} \tag{25}$$

$$E = k''_{Rs} \tag{26}$$

with

$$s = s' + is'' = a^{-2} \tag{27}$$

and

$$\sigma = (r^s_{pm})_{k_x=k_0} \tag{28}$$

$$k_{Rs} = k_{Rs} + ik''_{Rs} = -\frac{\omega}{c}(r^s_{pm})_{k_x=k_0}(\varepsilon_m \varepsilon_s)^{1/2}\frac{(\varepsilon_m + \varepsilon_s)^{1/2}}{(\varepsilon_m - \varepsilon_s)} \times \exp\left[i\frac{And}{A.}\left\{\frac{\varepsilon_m}{I\,(\varepsilon m + \varepsilon_s)^{1/2}}\right\}\right] \tag{29}$$

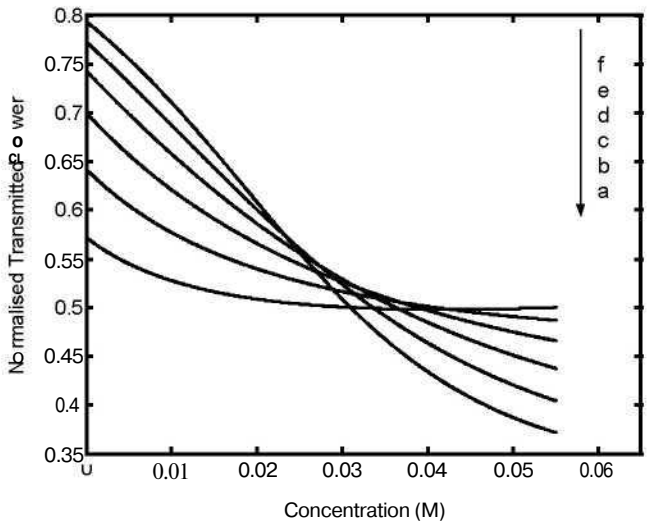

Fig. 3. Numerical simulations of transmitted power as a function of concentration of absorbing sample for optical absorption-based fiber optic SPR sensor for different values of frequency ω. (a) $\omega = \omega 0 - 0.75\gamma$, (b) $co = (Do - 0.5y$, (c) $co = COQ - 0.25y$, (d) $co = COQ$, (e) $co = COQ + 0.25y$ and (f) $\omega = \Omega 0 + 0.5\gamma$.

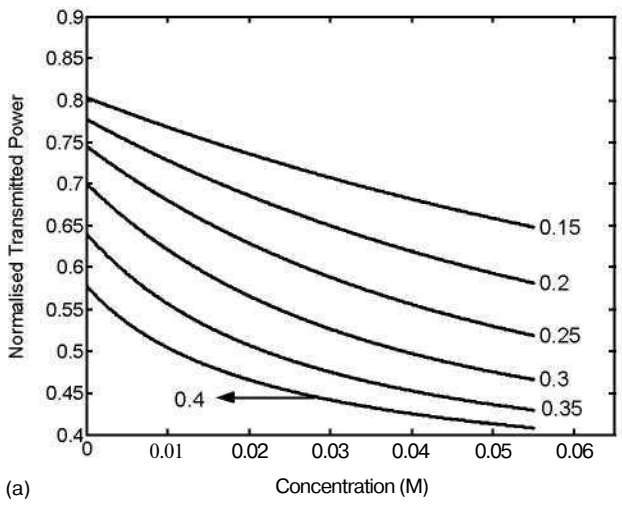

(a)

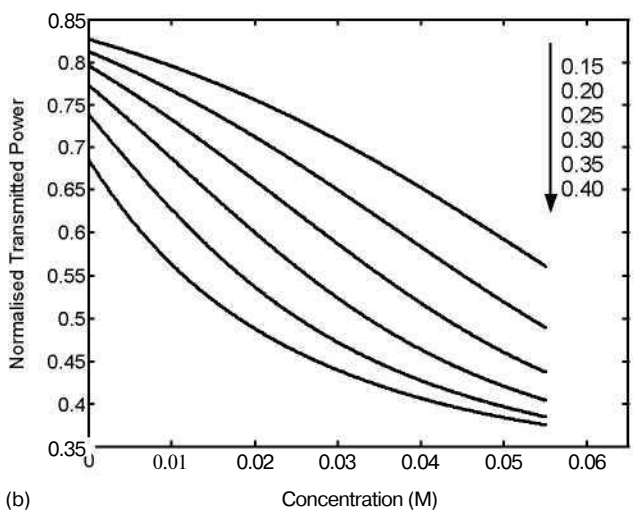

(b)

Fig. 4. Numerical simulations of transmitted power as a function of concentration of absorbing sample for optical absorption-based fiber optic SPR sensor for different numerical apertures of the fiber. (a) $\omega = \Omega 0$ and **(b)** $\omega < o)Q$.

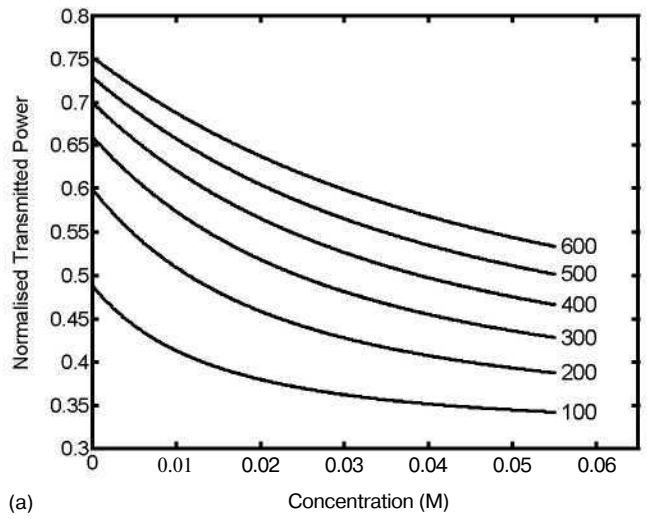

(a)

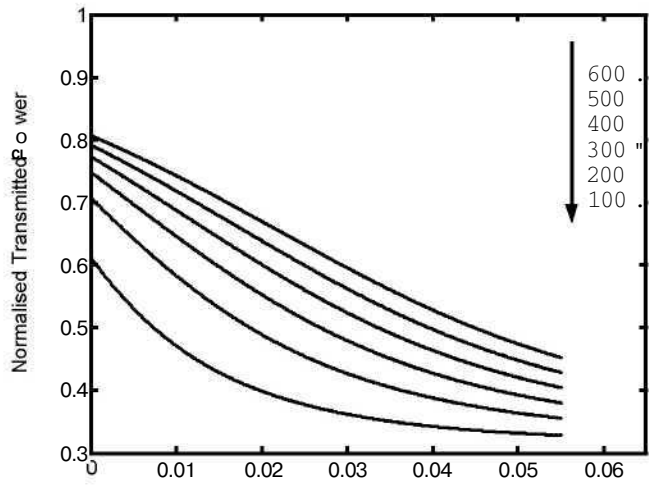

(b)

Fig. 5. Numerical simulations of transmitted power as a function of concentration of absorbing sample for optical absorption-based fiber optic SPR sensor for different values of the fiber core diameter (in [xm). (a) co = ω0 and (b) $\omega < \Omega 0$.

Both R_s (reflectance for s-polarization) and R_p (reflectance for p-polarization) contain k_x term in their respective expressions. Therefore, these reflectance are functions of the incident angle θ as k_x is a function of incident angle. In order to obtain the reflectance R for the un-polarized light, we simply take the mean of R_p and R_s [16], that is

$$R = \frac{R_p + R_s}{2} \quad \textbf{(30)}$$

2.2. Principle of the fiber optic SPR sensor

The optical absorption by the surface plasmon wave at the metal-sensing layer interface around the core of an optical fiber transmitting the light is the basis of the absorption-based fiber optic SPR sensor. Here the prism used in basic theory is replaced by the core of a plastic cladded optical fiber. The cladding around the core is removed from the middle portion of the fiber and is coated with a metal layer which is then surrounded by an absorbing fluid (Fig. 2). The light is launched into one of the ends of the fiber and is detected at the other end. The presence of the fluid and its concentration are determined by observing the change in the transmitted power. The normalized power transmitted depends on the extent of the optical absorption. In a fiber optic sensor, light is generally launched into a multimode fiber from a collimated source using a lens (microscope objective). The lens is used to focus the beam onto the fiber-end face at the axial point. The numerical aperture (NA) of the lens is larger than that of the fiber so that all the bound rays can be excited in the fiber. The power, dP, arriving at the fiber-end face between the angles θ_0 and θ0 + dθ0 is proportional to (tanθ0/cos^2 *Θ0)* dθ0, where *Θ0* is the angle of the ray from the axis for the ray outside the fiber. Using Snell's law and θ = 90° - θi, where θi is the

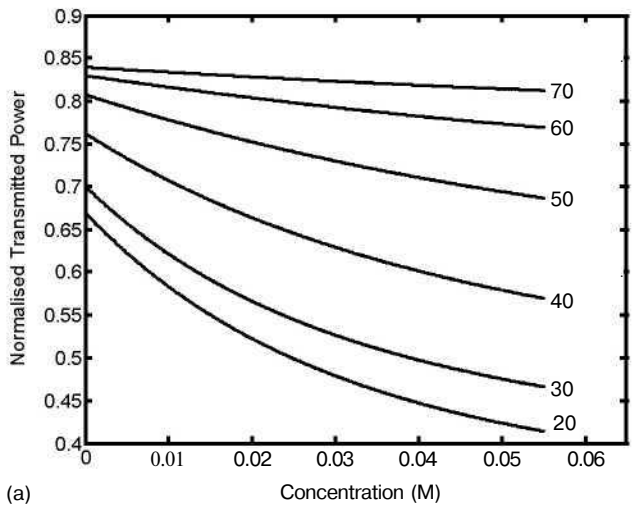

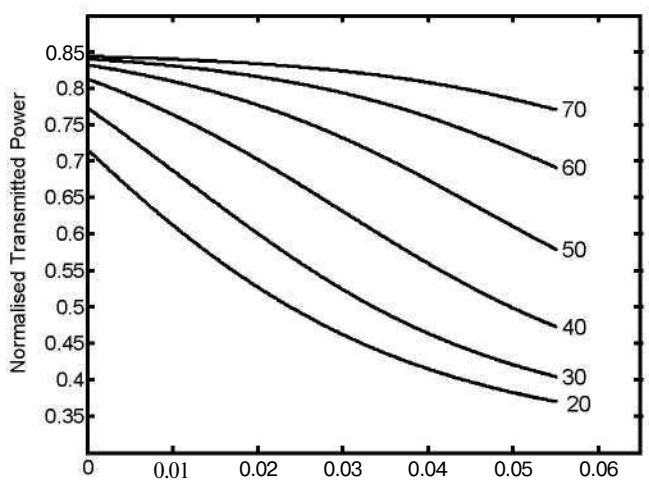

Fig. 6. Numerical simulations of transmitted power as a function of concentration of absorbing sample for optical absorption-based fiber optic SPR sensor for different values of film thickness (in nm). (a) $\omega = \omega 0$ and (b) $\omega < \omega 0$.

angle of the same ray from the axis of the fiber but inside the core, we can write [17]

$$dP \text{ a } \frac{n_1^2 \sin\theta\cos\theta}{(1-\text{«}^2\text{C}_1\text{OS}^2<9)^2} \text{d}\theta \quad \textbf{(31)}$$

Further the number of reflections, AW, in the fiber sensor area is a function of the mode propagation angle, θ, core diameter, D, and the length of the sensing area, L. This relationship is given by

$$\text{AW} = \text{—}^{L} = \quad (32)$$

In order to determine the effective transmitted power, the reflectance for a single reflection is raised to the power of the number of reflections the specific propagating angle undergoes with the sensor interface. Therefore, foranun-polarized collimated light source, the generalized expression for the normalized transmitted power, Ptrans, [m] an optical absorption based fiber optic SPR sensor is

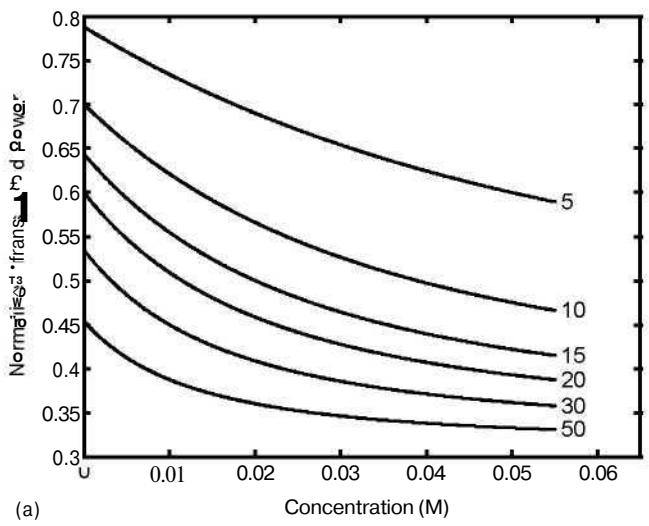

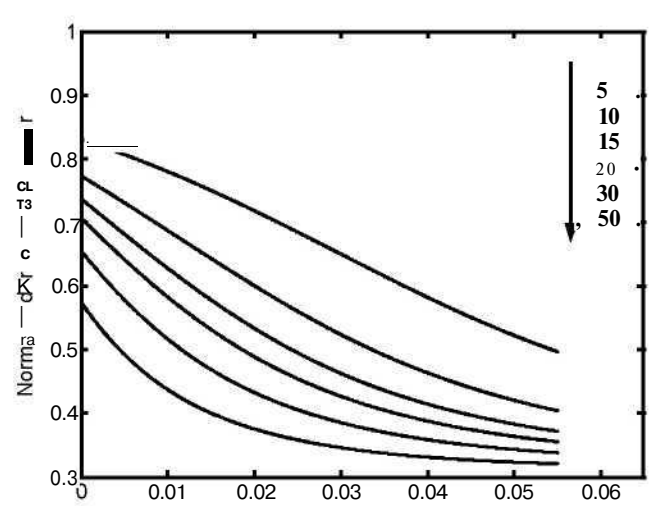

Fig. 7. Numerical simulations of transmitted power as a function of concentration of absorbing sample for optical absorption-based fiber optic SPR sensor for different lengths (in mm)of the SPR probe. (a) $\omega = \omega 0$ and (b) $\omega < \omega 0$.

$$\bar{r}_{\text{trans}} \equiv \frac{1}{\angle}\left[\frac{JZ^{\prime 2}\, {}_R N_{\text{re}}{}^{\text{gf}(\theta)}{}_{\text{tm}}(nf\sin 9\cos\theta/(1 - n21\cos^2\theta)^2)\text{d}\theta}{/cr^2(n12\sin\theta\cos\theta/(1 - n21\cos^2\theta)^2)\, d\theta} + \frac{\int^{\pi}/^2 RsNr^{\text{gf}(\theta)}(n21\sin\theta\cos\theta/(1 - n21\cos^2\theta)^2)d\theta}{\int_{\theta}^{3} l\backslash n\backslash \text{ sine cos } \theta/(1 - \text{«}_1^2\cos^2 0)^2)\text{de}}\right] \quad \textbf{(33)}$$

where

$$\theta_{cr} = \sin^{"1}\left(\text{n}\frac{n_{\text{cl}}}{n_1}\right) \quad \textbf{(34)}$$

is the critical angle of the fiber whereas $n_c l$ and n1 are the refractive indices of the cladding and core, respectively. Here we have neglected the polarization effect of different launched rays because in the SPR sensors the sensitive area

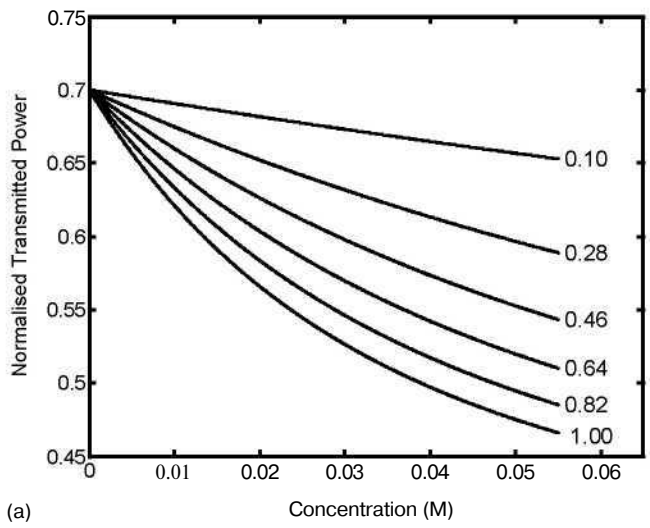

(a)

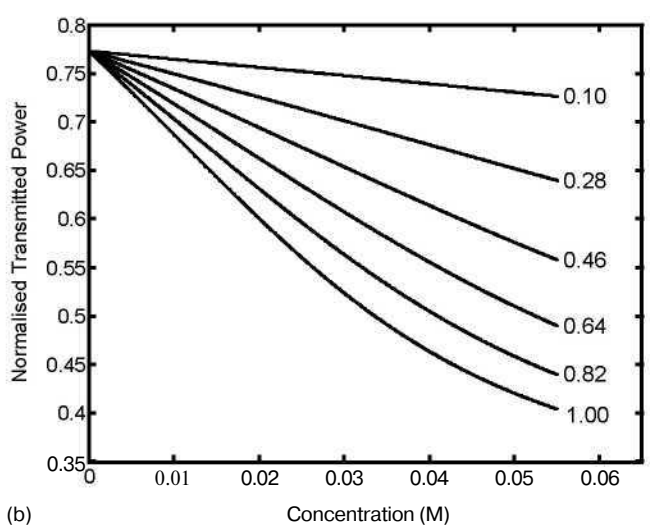

(b)

Fig. 8. Numerical simulations of transmitted power as a function of concentration of absorbing sample for optical absorption-based fiber optic SPR sensor for different values of the oscillator strength. (a) $\omega = \Omega 0$ and (b) $\omega < \Omega 0$.

is generally far from the input end of the optical fiber [18]. It is well known that the SPR phenomenon does not occur when the incident beam has a s-polarization. In Eq. (33), the second term corresponds to the normalized transmitted power for the s-polarized light when the absorption of light by the sensing layer is taken into account. However it is observed that in the presence of absorbing sensing layer the value of the second term is approximately equal to 0.68. This shows that the effect of absorption on the absorption based SPR phenomenon corresponding to s-polarization is constant. Thus Eq. (33) can be written as

$$P_{trans} = \frac{1}{2}\left[\frac{\int_{\theta_{cr}}^{\pi/2} N_{ref}(\theta)\,(\sin\theta\cos\theta/(0.68-w_1^2\cos^2\theta)^2)\,d\theta}{\int_{\theta_{cr}}^{\pi/2}(n_1^2\sin\theta\cos\theta/(1-n_1\cos^2\theta)^2)\,d\theta} + 1\right] \quad (35)$$

3. Results and discussion

To obtain the theoretical results, the optical parameters of Ag for the metal layer were used. For Ag the values of the parameters are e_m™ = 2.48, ω_p = 1.35 x 10^{16}rad/s, and ωd = 7.62 x 10^{13} rad/s. Further, the refractive index of the material of the fiber core has been taken as 1.48. The values of the other parameters used for calculations are: c = 2.998 x 10^{8}m/s, e = 1.602 x 10"^{19}C, m_e = 9.109x 10"^{31} kgandN_A = 6.02 x 10^{23} mol"^{1}. Fig. 3 shows the numerical simulations of transmitted power as a function of the molar concentration of the absorbing sample. The results have been plotted for different values of ω. The parameters used for these calculations are: D = 400 μm, N_A = 0.3, L = 10 mm, d = 30 nm, nf = 1.341, f = 1.0, λ_{max} = 600 nm and $\lambda\lambda_{max}$ = 100 nm. It can be seen from the figure that as the concentration increases the transmitted power received at the other end of the fiber decreases. The decrement depends on the relation between excitation frequency, ω, and the absorption frequency, $\omega 0$. For $\omega < \omega 0$ the sensitivity is more as compared *to* $\omega = \omega 0$ case. The sensitivity decreases for $\omega > \omega 0$ case. This result is different from the prism-metal surface-sensing layer combination. This is due to the fact that in the fiber all the guided rays have been launched and the results in Fig. 3 are due to all the angles. This suggests that for absorption based fiber optic SPR sensor one should choose $\omega < \omega 0$. Therefore to see the effect of fiber parameters, launching conditions and the probe geometry on the sensitivity of the sensor we shall consider only following two cases: $\omega = \omega 0$ and $\omega < \omega 0$.

3.1. Fiber parameters

Fig. 4(a) and **(b)** shows the effect of the numerical aperture of the fiber on the response characteristics of the sensor for $\omega = \omega 0$ and $\omega < \omega_0$, respectively. The numerical aperture is varied from 0.15 to 0.40. The other parameters remain same as in Fig. 3. It may be noted that the sensitivity of the sensor depends on the numerical aperture of the fiber in both the cases. It first increases then after attaining a maximum value it decreases. For the present case, the maximum occurs for the numerical aperture in the range 0.25-0.30. We have also studied the effect of fiber core diameter on the sensitivity of the SPR sensor. The simulation results are plotted in Fig. 5(a) and (b) for $\omega = \omega 0$ and $\omega < \omega 0$, respectively. The numerical aperture of the fiber was chosen as 0.30. For small core diameter fiber, the operating range of the sensor is small. The response curve starts saturating after C = 0.04 M concentration. For large value of core diameter the sensitivity and the operating range of the sensor are better.

3.2. Probe parameters

Metal film thickness and the length of the probe are the two important parameters of the SPR probe. Fig. 6(a) and (b) shows the effect of film thickness on the response

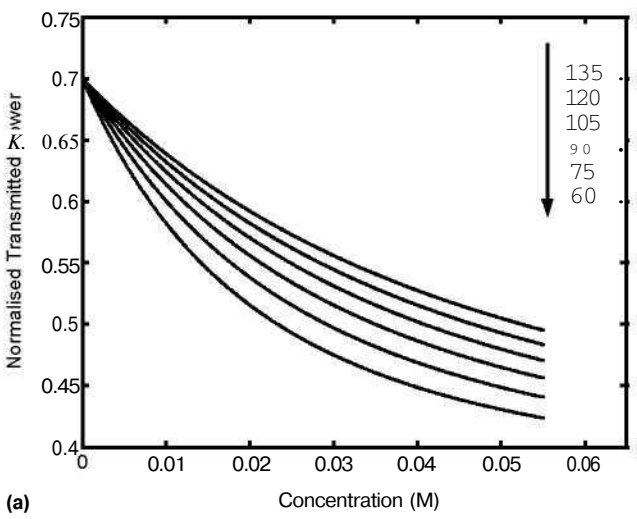

(a)

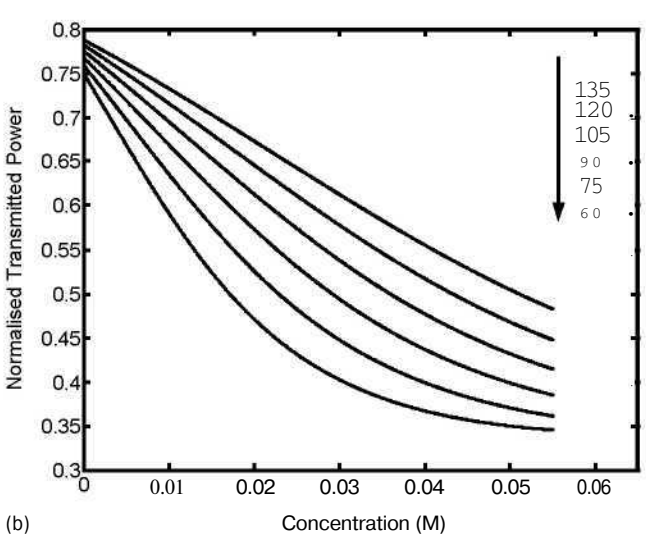

(b)

Fig. 9. Numerical simulations of transmitted power as a function of concentration of absorbing sample for optical absorption-based fiber optic SPR sensor for different widths (in nm) of the absorption spectrum of the oscillator. (a) $\omega = \Omega 0$ and (b) $\omega < \Omega 0$.

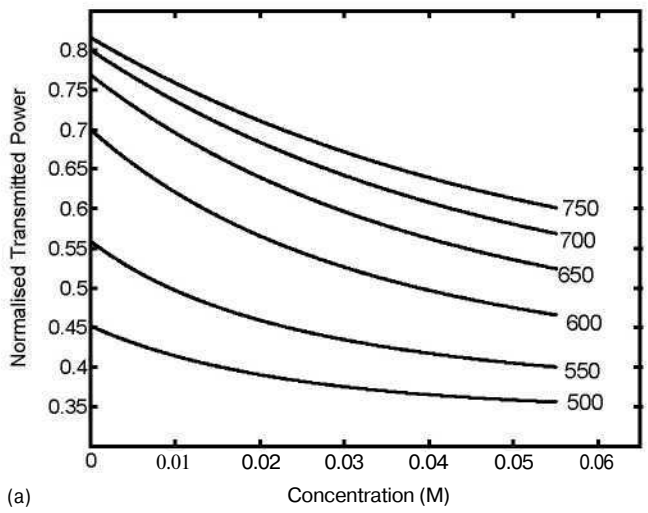

(a)

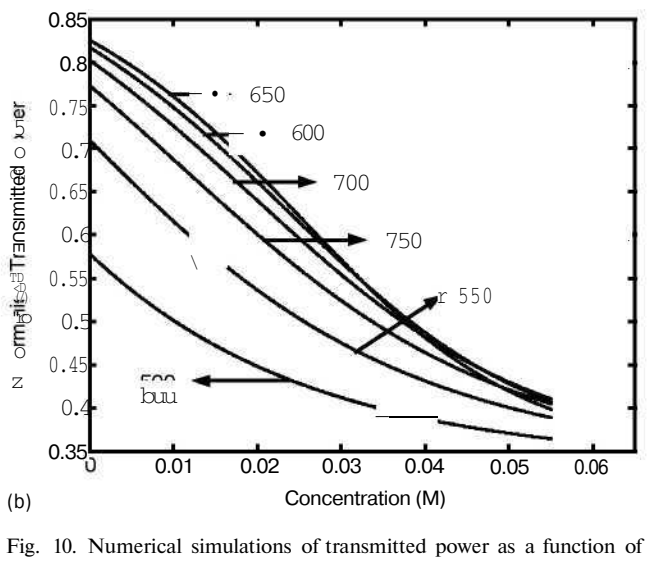

(b)

Fig. 10. Numerical simulations of transmitted power as a function of concentration of absorbing sample for optical absorption-based fiber optic SPR sensor for different absorption maximum wavelength (in nm) of the sample. (a) $\omega = \Omega 0$ and (b) $\omega < \Omega 0$.

curve of the sensor for $\omega = \omega 0$ and $\omega < \omega 0$, respectively. The results have been plotted for the fiber core diameter equal to 400 (xm. The film thickness is varied from 20 to 70 nm. It can be seen from the figures that the sensitivity is poor for large film thickness. For small thickness the sensitivity is high in the beginning but decreases after certain concentration thereby decreasing the operating range of the sensor. The best results are obtained for about 30-40 nm film thickness. The length of the probe also affects the sensitivity of the sensor. The sensitivity and the range of the sensor are optimum for $L = 10$ mm (Fig. 7(a) and (b)). Taking large length of the probe is not advantageous.

3.3. Sensing layer

Although Kurihara et al. [10] kept the value of oscillator strengthffixed at 1.0, we have tried to see the effect of extinction coefficient of the sensing layer by varying f from 0.1 to 1.0. The value offwas varied keeping other parameters constant. Fig. 8(a) and (b) show the effect offon the response curves of the SPR sensor for $\omega = \omega_0$ and $\omega < \omega_0$, respectively. It may be noted that, for a given concentration of the absorbing oscillators, an increase in the value of / increases the sensitivity of the sensor both the values of excitation frequency. However, the increase is more in the case *of* $\omega = \omega 0 - \gamma/2$. The sensitivity also increases with the decrease in the width of the absorption spectrum of the absorbing oscillator. This is shown in Fig. 9(a) and (b) for the value of $\lambda\lambda_{max}$ in the range of 60-135 nm. We have also studied the effect of λ_{max} on the response curves. The sensitivity is maximum around $\lambda\lambda_{max} = 650$ nm in the cases $co = \omega 0$ and $\omega = \omega_0 - \gamma/2$. It is more pronounced in the second case (see Fig. 10(a) and (b)). Finally, the effect of refractive index (n°) of the sensing layer on the sensitivity of the sensor was studied. Fig. 1 1(a) and (b) show the effect

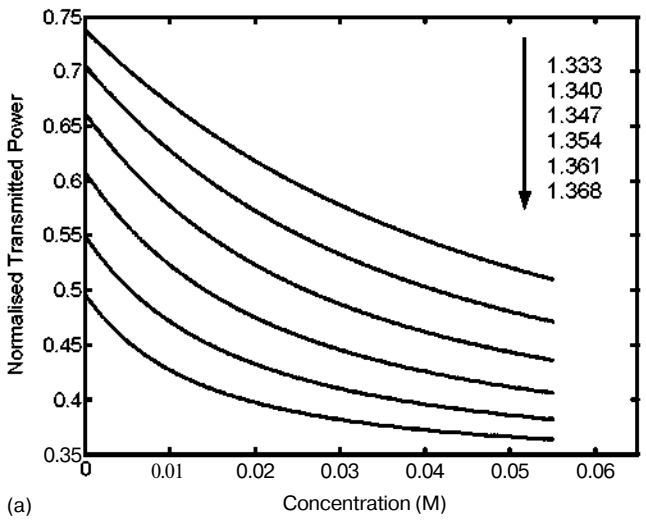

(a)

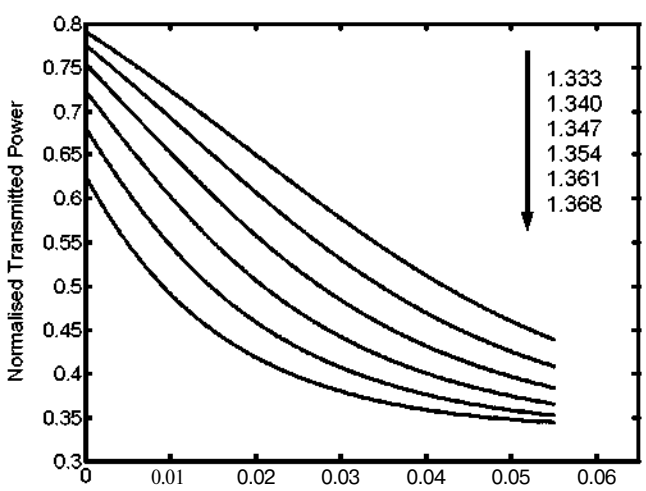

(b)

Fig. 11. Numerical simulations of transmitted power as a function of concentration of absorbing sample for optical absorption-based fiber optic SPR sensor for different values of the refractive index of the absorbing sample. (a) $\omega = \Omega 0$ and (b) $\omega < \Omega 0$.

of n° on the response curves. It can be seen that the sensitivity and the operating range of the SPR sensor is greater for small values of n_f°.

4. Conclusions

On the basis of these results following conclusions can be drawn:

(i) The excitation frequency in absorption-based fiber optic SPR sensor is an important parameter. A lower off-resonance excitation $(\omega = \omega 0 - \gamma/2)$ is recommended.

(ii) The fiber parameters affect the sensitivity of the sensor. There is an optimum range (0.25-0.30) of numerical aperture of the fiber for maximum sensitivity of the sensor. The sensitivity and the operating range of the sensor are better for large value of the core diameter. Hence a highly multimoded optical fiber is recommended.

(iii) The sensitivity of the sensor also depends on probe parameters such as metallic film thickness and its length along the fiber. The film thickness around 30 run and length about 1 cm give best results.

(iv) The increase in the extinction coefficient of the sample increases the sensitivity of the sensor while the decrease in the width of its absorption spectrum increases the sensitivity. The sensitivity and the operating range of the sensor are better for small values of the refractive index of the absorbing sample.

In summary, a new theoretical model has been presented that combines the sensitivity of absorption-based SPR with optical fiber technology. The fiber optic SPR probes based on our consideration will likely be developed for applications in analytical chemistry and biochemical and biomedical sensing because there may be a large number of analytes that may be sensed with the above concluded criteria.

Acknowledgements

One of the authors (AKS) is grateful to UGC for financial support.

References

[1] B. Liedberg, C. Nylander, I. Sundstrom, Surface plasmon resonance for gas detection and biosensing, Sens. Actuators 4 (1983) 299.
[2] S.L. Jung, C.T. Campbell, T.M. Chinowsky, M.N. Mar, S.S. Yee, Quantitative interpretation of the response of surface plasmon resonance sensors to absorbed films, Langmuir 14 (1998) 5636.
[3] E. Hutter, J.H. Fender, D. Roy, Surface plasmon resonance studies of gold and silver nanoparticles linked to gold and silver substrates by 2-amino-ethanethiol and 1,6-hexanedithiol, J. Phys. Chem. B 105 (2001) 11159.
[4] J. Homola, S.S. Yee, G. Gauglitz, Surface plasmon resonance sensors: review, Sens. Actuators B 54 (1999) 3.
[5] Z. Salamon, H.A. Macleod, G. Tollin, Surface plasmon resonance spectroscopy as a tool for investigating the biochemical and biophysical properties of membrane protein systems. I: Theoretical principles, Biochim. Biophys. Acta 1331 (1997) 117.
[6] Z. Salamon, H.A. Macleod, G. Tollin, Surface plasmon resonance spectroscopy as a tool for investigating the biochemical and biophysical properties of membrane protein systems. II: Applications to biological systems, Biochim. Biophys. Acta 1331 (1997) 131.
[7] E. Kretchmann, H. Reather, Radiative decay of non-radiative surface plasmons excited by light, Naturforsch. 23 (1968) 2135.
[8] A. Otto, Exitation of nonradiative surface plasma waves in silver by the method of frustrated total reflection, Z. Phys. 216 (1968) 398.
[9] E. Kretchmann, Die Bestimmung optischer Konstanten von Metallen durch Anregung von Oberflachenplasmashwingungen, Z. Phys. 241 (1971) 313.
[10] K. Kurihara, K. Suzuki, Theoretical understanding of an absorption-based surface plasmon resonance sensor based on Kretchmann's theory, Anal. Chem. 74 (2002) 696.

[11] K. Kurihara, K. Nakamura, K. Suzuki, Asymmetric SPR sensor response curve-fitting equation for the accurate determination of SPR resonance angle, Sens. Actuators B 86 (2002) 49.
[12] R.C. Jorgenson, S.S. Yee, A fiber-optic chemical sensor based on surface plasmon resonance, Sens. Actuators B 12 (1993) 213.
[13] R.C. Jorgenson, C. Jung, S.S. Yee, L.W. Burgess, Multi-wavelength surface plasmon resonance as an optical sensor for characterizing the complex refractive indices of chemical samples, Sens. Actuators B 14 (1993) 721.
[14] J. Homola, Optical fiber sensor based on surface plasmon resonance, Sens. Actuators B 29 (1995) 401.
[15] W.B. Lin, M. Lacroix, J.M. Chovelon, N. Jaffrezic-Renault, H. Gagnaire, Development of a fiber-optic sensor based on surface plasmon resonance on silver film for monitoring aqueous media, Sens. Actuators B 75 (2001) 203.
[16] M. Born, E. Wolf, Principles of Optics, sixth ed., Section 1.5, Pergamon Press, Oxford, 1987.
[17] B.D. Gupta, A. Sharma, C.D. Singh, Evanescent wave absorption sensors based on uniform and tapered fibers, Int. J. Optoelectron. 8 (1993) 409.
[18] W.B. Lin, N. Jaffrezic-Renault, A. Gagnaire, H. Gagnaire, The effects of polarization of the incident light-modeling and analysis of a SPR multimode optical fiber sensor, Sens. Actuators A 84 (2000) 198.

Biographies

Anuj K. Sharma received his MSc degree in physics (2001) from Indian Institute of Technology, Roorkee (India). Since April 2002, he is a full time PhD student at the Physics Department, Indian Institute of Technology, Delhi. Mr. Sharma has been selected for UGC (India) research fellowship in 2001.

B.D. Gupta received his BSc (Hons.) (1973) and MSc degree in physics (1975) from Aligarh Muslim University (India) and a PhD degree in physics (1979) from the Indian Institute of Technology, New Delhi. In 1978 he joined the Indian Institute of Technology, New Delhi, where he is currently an assistant professor of physics. Dr. Gupta has also worked at the University of Guelph (Canada) in 1982-1983, the University of Toronto (Canada) in 1985, and the Florida State University (USA) in 1988. In 1993, he visited the Department of Electronic and Electrical Engineering at the University of Strathclyde (UK) to work on fiber optic chemical sensors under the Indo-British Fibre Optics Project. In 1992, he was awarded the ICTP Associateship by the International Centre for Theoretical Physics, Trieste (Italy), which he held for eight consecutive years. In this capacity, he visited ICTP (Italy) in both 1994 and 1996. Dr. Gupta is a recipient of the 1991 Gowri Memorial Award of the Institution of Electronics and Telecommunication Engineers (India). He has published more than 50 research papers including four review articles. Dr. Gupta is the co-editor of *Asian Journal of Physics*, *Proceedings of SPIE (USA)* (vol. 3666) (1998) and *Advances in Contemporary Physics and Energy* (Supplement Volume) (Allied Publishers, New Delhi). His current area of interest is fiber optic sensors. He is a life member of the Optical Society of India and the Indian Chapter of ICTP.